energy&fuels

Article

pubs.acs.org/EF

Influence of Support Acidity and Ir Content on the Selective Ring Opening of Decalin over $Ir/SiO_2-Al_2O_3$

Silvana A. D'Ippolito, Adriana D. Ballarini, and Carlos L. Pieck*

Instituto de Investigaciones en Catálisis y Petroquímica (INCAPE) (FIQ-UNL, CONICET), Colectora Ruta Nac. No. 168, Paraje El Pozo, CP 3000, Santa Fe, Argentina

Supporting Information

ABSTRACT: The influence of the addition of HCl and Ir (1 wt %) to different $SiO_2-Al_2O_3$ supports of varying silica content was studied in the reaction of selective ring opening of decalin. The addition of HCl to silica−alumina supports containing 70 and 80 wt % SiO_2 was found to have little influence in the distribution of reaction products compared to the calcined supports. The incorporation of Ir to the silica−alumina catalysts has a beneficial effect, increasing the decalin conversion, being this effect more noticeable in the low acidity supports, i.e., those containing 30−40 wt % SiO_2. The iridium-containing materials display the highest yield of cracking products, ring opening products, and ring contraction products. Increasing the reaction temperature promotes cracking and dehydrogenation but markedly decreases the selectivity to ring contraction products. At 350 °C a slight decrease in selectivity to ring opening products occurs, though the overall increase in conversion results in an increased yield of these products. An optimum ratio between the acid sites and metal activity that favors the formation of ring opening products was found. At lower acid sites/metal activity ratios the isomerization reaction which leads to C_5 cycle isomers is low, and ring opening by hydrogenolysis is limited as a consequence. On the other hand, at high acid sites/metal activity ratios the cracking reactions are favored, decreasing the yield of RO products.

INTRODUCTION

The need to produce diesel from heavy refinery fractions with molecules containing multiple condensed aromatic and naphthenic rings has generated a sustained interest in developing catalysts and processes for selective ring opening (SRO). Selective ring opening of naphthenic molecules is a promising reaction for the upgrading of low-value streams issuing from some refinery units, as it is the case of light cycle oil (LCO), a residual stream of the fluid catalytic cracking (FCC) units.[1,2] Calemma et al.[3] found that the results obtained in the catalytic hydroconversion of desulfurized and dearomatized LCO were in agreement with the results obtained using decalin as a model molecule. The cetane number (CN) was found to increase significantly when decalin was converted to linear or monobranched paraffins. CN is one key quality parameter in diesel fuel, with high cetane values ensuring proper combustion and low emissions of NO_x and particulates.[4]

A large number of publications postulate that the SRO mechanism starts with the saturation of the aromatic ring, followed by isomerization, ring opening, and eventually cracking.[5−8] In more detail, Resasco et al.[9] showed that the opening reaction of decalin is catalyzed by the acid function via β-cleavage and by the metal function via a dicarbene mechanism leading to highly isomerized products. Moraes et al.[10] proposed another mechanism for the ring contraction reaction, mainly according to a bifunctional mechanism. For ring opening reactions a direct path and an indirect path were considered. The direct path takes place on metal sites, while the indirect path produces ring contraction products on acid sites that can be opened on the metal sites according to a bifunctional mechanism. Bifunctional catalysts that combine a metal with high hydrogenolytic activity and a support with acid sites have shown good performance for SRO of decalin.[11,12]

Studies performed on metallic Ir, Pt, Ru, and Rh supported catalysts have determined that the hydrogenolytic capacity follows the order Pt < Rh < Ir < Ru,[13,14] with Ir being the most selective toward ring opening products.[5] The ring opening capacity has also been found to be affected by the size of the metal particles,[13] the nature of the support,[15] and the naphthenic compound.[5,16] Nassreddine et al. have determined that the selectivity ratio between ring opening/ring contraction products increases at higher acid/metal site ratios. This phenomenon was observed using several silica−alumina supports with different compositions, metal particle sizes, and Ir contents.[8,17]

Some other studies have however tried to limit the strength and concentration of the Brønsted acid sites (involved in the isomerization of six to five membered naphthenic rings which are easier to break by hydrogenolysis) by incorporating alkali metal cations to reduce the extent of undesired cracking reactions.[3,18,19] Rabl et al.[18] studied decalin ring opening using zeolite-based catalysts Ir/La-X and Pt/La-X. The acid sites were created by ionic exchange with La^{3+} followed by thermal drying. They concluded that the strength of the Brønsted sites formed increases in the following order: Cs,HY < Rb,HY < K,HY < Na,HY < Li,HY.[20] They also reported that since the acid activity of the bifunctional catalysts is relatively low, the undesired hydrocracking to C_9 products can be kept at a low

Received: February 14, 2017
Revised: March 20, 2017
Published: March 29, 2017

ACS Publications © 2017 American Chemical Society

DOI: 10.1021/acs.energyfuels.7b00451
Energy Fuels 2017, 31, 5461−5471

level, thereby enabling unusually high yields of open-chain C_{10} products.[20]

The choice of the support has been found to greatly influence the SRO activity. Interaction of the support with the metal particles changes the electronic properties of the metal, while the presence of acid sites can significantly change the reaction mechanism.[21] Several researchers have proposed to use zeolites as supports due to their high amount of Brønsted acid sites that favors the bifunctional mechanism.[6,20,22] Amorphous silica−alumina containing mixed phases of silica−alumina, pure silica, and alumina groups were also studied for SRO of decalin[23−25] because silica−alumina has Brønsted acid sites with a strength similar to those of zeolites but their concentration is lower and can be further adjusted by varying the silica content.[26]

One desired effect is the interaction between metals and acid supports that can promote the resistance of the catalyst to sulfur compounds in the feed. Electron transfer from the metal to the support weakens the metal−sulfur bond and disfavors strong chemisorption of sulfur-containing molecules.[1,8] Several works on SRO have studied the combination of the hydrogenolytic capacity and thio tolerance of iridium and the ring contraction properties of the acid sites.[9,27] As a drawback, Ir addition has been found to decrease the amount of Brønsted strong acid sites.[10]

In this work the effect of the addition of HCl and iridium to SiO_2−Al_2O_3 catalysts was studied. Materials with different contents of SiO_2 (30, 40, 60, 70 and 80% by weight) were promoted with Ir and in some cases with HCl, and their activity and selectivity in the selective opening of decalin were studied. Reaction temperature was also varied. A focus was put on the search for optimal preparation and reaction conditions for maximizing the liquid yield and the selectivity to high cetane products.

EXPERIMENTAL SECTION

Catalyst Preparation. Commercial SiO_2−Al_2O_3 was provided by SASOL (SIRAL 30, 40, 60, 70, and 80). Samples of 5 g of these materials were calcined for 4 h in air (450 °C, 60 cm^3 min^{-1}). The heating rate from room temperature to the final one was 10 °C min^{-1}. Each calcined support was named S*x*, with *x* indicating the weight percent of SiO_2 in the silica−alumina support.

Addition of HCl. A 5 g sample of the calcined support was impregnated with 7.5 cm^3 of HCl (0.2 M) and left unstirred for 1 h. Then it was dried at 70 °C in a thermostatic bath until a dry powder was obtained. The product obtained was left overnight in an oven at 120 °C. Finally it was calcined in flowing air (60 cm^3 min^{-1}, 300 °C, 4 h). The heating rate used was 10 °C min^{-1}. These supports were named HCl/S*x*.

Preparation of Iridium Supported Catalysts. The HCl/S*x* supports were further impregnated with a solution of the metal precursor salt (H_2IrCl_6, 0.014 M aqueous solution) in order to obtain 1 wt % Ir in the final catalyst. The obtained slurry was stirred gently for 1 h. Then the samples were dried following the aforementioned procedure. Then the catalysts were heated at 10 °C min^{-1} to 500 °C in flowing hydrogen (60 cm^3 min^{-1}) and reduced at this temperature for 4 h. After cooling to room temperature the samples were blanketed in nitrogen for storage. These catalysts were named Ir/S*x*.

Catalyst Characterization. The metal content was determined by inductively coupled plasma optical emission spectroscopy (ICP-OES) after digesting the catalyst in an acid solution. The chloride content of the catalysts was determined by the Volhard−Charpentier method.

A Shimadzu XD-D1 diffractometer operated at 30 kV and 40 mA and using Cu Kα radiation filtered with Ni was used to scan the 10−70° range at a rate of 2° min^{-1}.

Transmission electron microscopy (TEM) measurements were carried out on a JEOL 100CX microscope, operated with an acceleration voltage of 100 kV. For each catalyst, approximately 200 Ir particles were observed and the distribution of particle sizes was measured. The mean particle diameter (d_p) was calculated as

$$d_p = \frac{\sum n_i d_i^3}{\sum n_i d_i^2}$$

where n_i is the number of particles of diameter d_i.

The dispersion was estimated as the ratio between the theoretical minimum particle diameter and the apparent particle diameter measured by TEM according to the method of Kubicka.[28]

Dispersion was also determined by dynamic chemisorption of CO. Calibrated pulses of the adsorbate were injected in a stream of nitrogen that flowed over the sample. These pulses were sent to the reactor until the sample was saturated. At the beginning of the experiment, the sample (150 mg) was reduced at 500 °C (10 °C min^{-1}) for 1 h. Then, nitrogen was made to flow over the sample for 1 h at 500 °C in order to eliminate adsorbed hydrogen. Then the sample was cooled to room temperature in nitrogen and pulses of 0.6 μmol of CO were sent to the reactor.

Temperature-programmed-reduction (TPR) experiments were carried out at atmospheric pressure using a reductive mixture of H_2:N_2 (5% H_2 v/v, 10 cm^3 STP min^{-1}). Catalyst samples (200 mg) were heated at 10 °C min^{-1} from 25 to 750 °C. The TPR signal was produced by a thermal conductivity detector (TCD). Before the TPR measurements, the samples were calcined "in situ" at 400 °C with flowing air (160 cm^3 min^{-1} g of cat^{-1}) for 1 h. The heating rate was 10 °C min^{-1}.

The acidity of the supports and catalysts was assessed by means of temperature-programmed desorption (TPD) of pyridine. Samples of 200 mg were impregnated with an excess of pyridine. The samples were then rinsed and the excess of physisorbed pyridine was eliminated by heating the sample under nitrogen flow at 110 °C for 1 h. For desorption the temperature was raised to 850 °C at a heating rate of 10 °C min^{-1}. Desorbed pyridine in the reactor exhaust was measured using a flame ionization detector (FID). The total amount of adsorbed pyridine was determined by comparing the area of the TPD traces with the area produced by calibrated pyridine pulses (1−2 μL) injected to the empty reactor. The error associated with the peak position and areas has been determined to be of about 7%.[29]

Cyclopentane (CP) hydrogenolysis and ring opening of methylcyclopentane (MCP) were used as test reactions of the metal and acid functions of the catalysts. Both reactions were performed at atmospheric pressure in a glass reactor (length = 10 cm, diameter = 1 cm). The catalyst was placed over a porous glass support. The liquid reactives were introduced by the use of a needle pump, while the hydrogen flow rate was controlled by a mass flow controller. Both were injected at the top of the reactor and flowed cocurrently to the bottom where a sampling valve was used to collect samples. Before the reaction, catalyst samples were reduced with H_2 at 500 °C for 1 h. The conditions used were the following: catalyst mass = 80 mg, H_2 flow rate = 36 cm^3 min^{-1}, MCP and CP flow rate = 0.36 cm^3 h^{-1}, weight hourly space velocity of cyclopentane ($WHSV_{CP}$) = 3.38 h^{-1}, $WHSV_{MCP}$ = 3.37 h^{-1}, reaction temperature = 250 °C, and reaction time = 2 h. The heating rate to the reaction temperature was 10 °C min^{-1} for both reactions. The products were analyzed on a Varian CX 3400 gas chromatograph (GC) equipped with a capillary Phenomenex ZB-1 column. The absence of mass transfer limitations was determined by calculating the Weisz−Prater modulus and the Damköhler number for the CP and MCP reactions. In all cases the Weisz−Prater modulus was found to be much smaller than 0.1 while the Damköhler number was smaller than 0.01.[30]

The reaction of decalin was used to test the activity for selective ring opening. A stainless steel autoclave reactor was used. A 1 g sample of catalyst was put in contact with 25 cm^3 of decalin (37.5% cis isomer and a trans/cis ratio of 1.63) at 325 or 350 °C, at a hydrogen pressure of 3 MPa and with a stirring rate of 1360 rpm. At these reaction conditions, the catalyst was reduced to powder by attrition after a few

DOI: 10.1021/acs.energyfuels.7b00451
Energy Fuels 2017, 31, 5461−5471

minutes. The powder obtained after 5 min could pass through a 200 mesh sieve. This particle size ensured that diffusional limitations to mass transfer were eliminated. Product identification studies were performed by GC−MS in a Saturno 2000 mass spectrometer (MS) coupled to a GC Varian 3800 using the same GC column.

RESULTS AND DISCUSSION

The specific surface area and the chemical composition of the supports provided by SASOL are presented in Table 1. The S30 had the lowest surface area, while the S40 had the largest. Supports with a SiO_2 content above 39 wt % presented lower surface areas as the SiO_2 load increased.

Table 1. Main Characteristics of the Supports Studied

characteristic	S30	S40	S60	S70	S80
Al_2O_3 (%)	69.8	60.7	42.6	28.5	21
SiO_2 (%)	30.2	39.3	57.4	71.5	79
sp surf. area ($m^2\ g^{-1}$)	183	514	489	377	337
apparent density ($g\ cm^{-3}$)	0.32	0.33	–	0.21	0.24

X-ray diffractograms for all the studied supports are shown in Figure 1. It can be seen that all the samples displayed a halo at

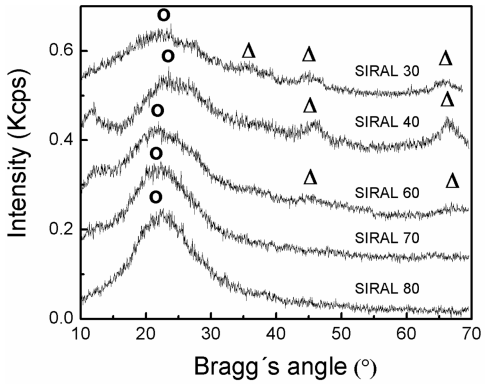

Figure 1. X-ray diffractograms of the calcined supports. (△) Al_2O_3; (○) SiO_2.

2θ = 23−24°, characteristic of amorphous silica−alumina.[31] The X-ray diffractogram of SIRAL 40 has been previously published,[24] and it has been included in Figure 1 for comparison. The diffraction peaks at about 37.5, 39.6, 46, and 67.4° could be attributed to γ-Al_2O_3.[32,33]

The presence of diffraction peaks due to SiO_2 and Al_2O_3 demonstrates that both phases exist separately in S30, in S40, and to a lesser extent in S60. Increasing the silica content produces a remarkable growth of the halo at 2θ = 20−30° which is due to the SiO_2 amorphous phase. Moreover, the diffraction peaks of Al_2O_3 decrease and practically disappear in the case of the S70 and S80 supports.

Table 2 shows the values of Ir and Cl contents as well as the mean particle size and the metallic dispersion as determined by TEM and by CO chemisorption (TEM images of the catalysts are shown in the Supporting Information, Figures 1S−5S). Table 2 shows that the percentage of Ir determined by ICP differs by 4−12% from the theoretical value. Generally speaking, it can be said that deposition of Ir does not have any correlation with the support acidity (see Table 3) or specific surface area, even though the lowest amount of Ir deposited occurred on the support with the lowest surface area (S30). The metallic dispersion obtained by TEM and by CO

Table 2. Chlorine and Iridium Concentrations and Mean Particle Size As Determined by TEM: HCl/S*x* and Ir/S*x* Catalysts

				metallic dispersion (%)	
catalyst	Cl (wt %)	Ir (wt %)	particle size (nm)	by TEM	by CO
HCl/S30	0.87	–			
Ir/S30	0.74	0.88	2.7	34	37
HCl/S40	0.93	–			
Ir/S40	0.79	0.89	2.3	40	43
HCl/S60	0.96	–			
Ir/S60	0.84	0.94	2.2	42	44
HCl/S70	0.89	–			
Ir/S70	0.76	0.93	2.1	44	45
HCl/S80	0.72	–			
Ir/S80	0.61	0.96	2.4	38	41

chemisorption were very similar, but the values determined by CO chemisorption are slightly higher. It can also be seen in Table 2 that the mean particle diameters of the Ir catalysts were similar, though Ir/S30 showed the largest diameter.

The poor metallic dispersion of Ir/S30 could be due to the low specific surface area of the support.[34] The fact that iridium species are weakly bonded to the support due to their low acidity must also be considered. As a consequence, iridium species could have migrated during the reduction step of the catalyst preparation.[35] The chlorine contents show that the HCl/S*x* series had a Cl content about 15% higher than the Ir/S*x* series.

A pyridine TPD trace scan supplies information on the strength and concentration of different surface acid sites. According to the desorption temperature, the acid sites can be classified as weak (T < 300 °C), moderate (300 < T < 500 °C), and strong (T > 500 °C). S30 had mainly moderate acidity sites as seen in Figure 2 and Table 3. The other supports had mostly moderate and strong acid sites, except for S60 that had a higher amount of weak acid sites than strong acid sites.

The impregnation of the support with chlorine increased the total acidity by 20−30% as compared to the nonchlorinated supports. However, the acid distribution was similar for both kinds of supports. This acidity increase due to Cl addition has been previously reported for Al_2O_3 and SiO_2.[36,37] The incorporation of Ir also increased the total acidity. Mainly new strong acid sites were created. It can be seen that, in all cases, the incorporation of Ir increased the total acidity, the amount of strong acid sites of each support, and, to a lesser extent, the concentration of moderate acid sites. In the case of the S60 support the amount of strong acid sites created was higher.

Although FTIR-Py results are often considered more precise, Selli et al.[38] reported that TPD-Py and FTIR-Py techniques showed good agreement when the total acidity is measured at equilibrium conditions at 150 °C (Fourier transform infrared (FTIR) measurements) and kinetic control (TPD). A direct correlation between both techniques was found for Ir/S70 and Rh/S70 catalysts (data not shown). The total acidity ratio determined by TPD between the SIRAL 70 and 80 supports was 1.01, while the ratio measured by FTIR-Py was 1.06 (at 150 °C). Also, the total acidity ratio for Rh(1.0)/S70 catalyst compared to Ir(1.0)/S70 was 1.11 measured by both techniques.

DOI: 10.1021/acs.energyfuels.7b00451
Energy Fuels 2017, 31, 5461−5471

Table 3. Total Acidity and Acid Strength Distribution As Obtained from Pyridine (Py) TPD Tests

		acid amount (μmol of Py g^{-1})		
catalyst	total acidity (μmol of Py g^{-1})	weak (<300 °C)	moderate (300 < T < 500 °C)	strong (>500 °C)
S30	479	38	422	19
S40	673	38	322	313
S60	1559	251	1161	147
S70	1119	128	493	498
S80	1104	303	384	417
Ir/S30	739	47	398	294
Ir/S40	953	28	427	498
Ir/S60	2535	85	725	1725
Ir/S70	1763	95	564	1104
Ir/S80	1820	85	626	1109

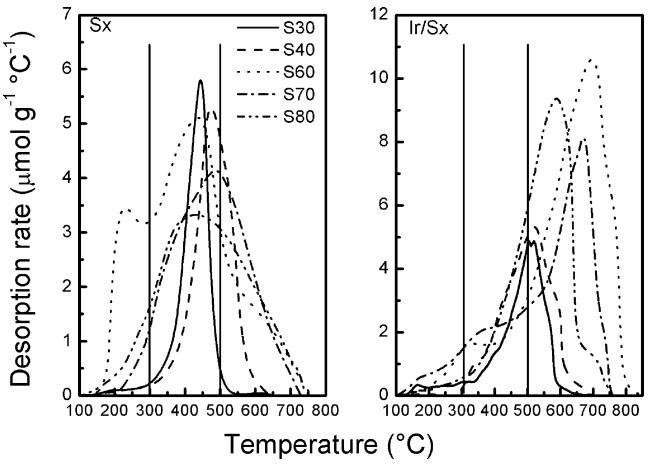

Figure 2. Pyridine TPD profiles of calcined supports and Ir/S*x* catalysts.

Figure 3 shows the TPR traces of the Ir supported catalysts. The TPR surface area shows that all Ir was reduced to the zero valence metal state. The reduction peaks can be attributed to the reduction of iridium oxide and iridium chloride species with different degrees of interaction with the support. It can be seen that the iridium oxides were reduced at increasingly lower temperatures as the SiO_2 content increased, except for Ir/S80 which had a higher reduction temperature than Ir/S70. This is in agreement with a lower reduction temperature reported for Ir oxides supported on SiO_2 compared to Ir/Al_2O_3.[39] Ir supported on S30, S40, and S60 displayed big reduction peaks at 243−276 °C with a long tail. The broad reduction peaks put in evidence the great heterogeneity of the Ir surface oxides. The TPR traces of Ir/S70 and Ir/S80 showed two reduction peaks and a long tail. The pattern of these TPR traces could be explained by recalling that large particles are reduced at a lower temperature than well-dispersed oxide species.[40,41] However, the metal particle size distributions and mean particle sizes (Table 2) as obtained by TEM do not support this hypothesis.

The cyclopentane hydrogenolysis reaction demands an ensemble of metal atoms with a given configuration. Therefore, the reaction product distribution depends on the metal particle size distribution.[42,43] An influence of the particle size on the hydrogenolysis reaction could not be observed because all Ir catalysts had similar metal particle sizes (Table 2). Table 4 shows that the turnover frequency (TOF, molecules of CP converted per unit Ir surface atom per second) was of the same order of magnitude (0.48−0.66 s^{-1}) for all Ir catalysts. Figure 4 shows that the activity increased with metal content. Deep

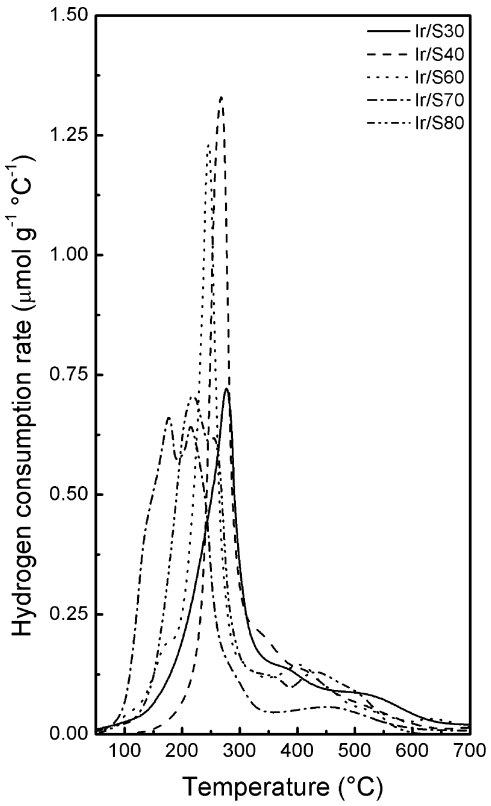

Figure 3. TPR results. Ir/S*x* catalysts.

Table 4. Turnover Frequency (TOF, s^{-1}) of Cyclopentane Hydrogenolysis and Methylcyclopentane Ring Opening Reactions: Ir/S*x* Catalysts

catalyst	TOF CP (s^{-1})	TOF MCP (s^{-1})
Ir/S30	0.56	0.51
Ir/S40	0.48	0.45
Ir/S60	0.48	0.46
Ir/S70	0.58	0.38
Ir/S80	0.66	0.51

hydrogenolytic activity, i.e. methane formation, followed the same trend. On the other hand, since the reaction is catalyzed by the metal sites, the reaction rate and the selectivity to methane were not directly proportional to the total acidity or strong or medium acid sites of the catalysts (results not shown). The selectivity to all reaction products detected for the

DOI: 10.1021/acs.energyfuels.7b00451
Energy Fuels 2017, 31, 5461−5471

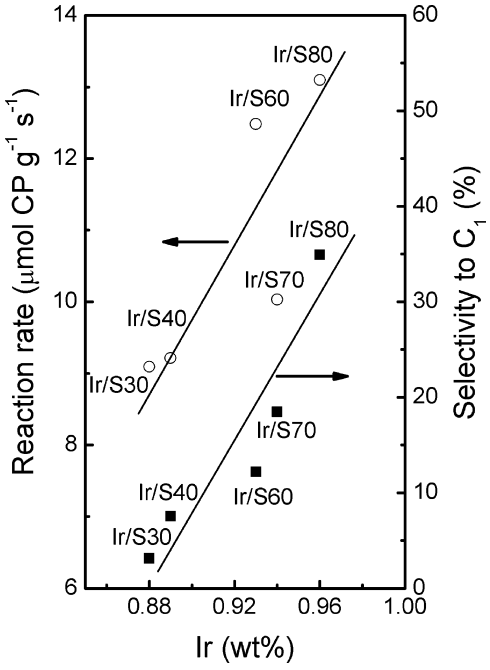

Figure 4. Reaction rate of cyclopentane (○) and selectivity to C_1 (■) extrapolated to zero reaction time.

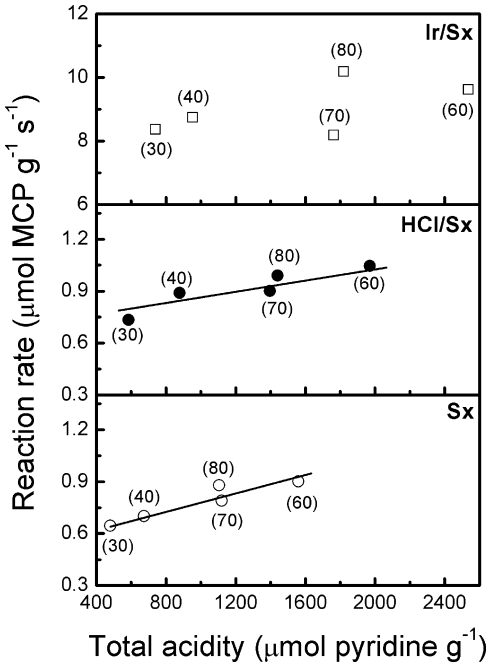

Figure 5. Reaction rate of methylcyclopentane as a function of total acidity of the catalysts. Numbers in parentheses identify the support.

cyclopentane reaction is available as Supporting Information (Table 1S).

In order to study the methylcyclopentane (MCP) ring opening reaction, the reaction products were classified according to the definitions given by Djeddi et al.[44] This includes cracking products (C_1−C_5), ring opening products (RO: 2-methylpentane, 3-methylpentane, and *n*-hexane), isomerization or ring enlargement products (cyclohexane), and dehydrogenation products (benzene). As expected due to the small difference in metal particle size, the turnover frequency (molecules of MCP converted per Ir surface atom per second) had only slight variations (Table 4). However, before drawing a conclusion, the influence of the acid function must be analyzed, too.

Figure 5 shows the reaction rate of methylcyclopentane as a function of the total acidity for the three studied series. It can be seen that in the S*x* and HCl/S*x* series the reaction rates increased with the total acidity. Although it is well-known that the reaction is catalyzed by the metal sites [ref 45 and references therein], these results showed that acid sites can also catalyze the reaction. In all cases the support with chlorine had more activity than the corresponding support without chlorine. In the case of the Ir catalysts, the reaction rate also increased with the total acidity but there are some points that did not follow this trend. Also, the conversion was increased by an order of magnitude by the addition of Ir. The high and anomalous conversion values could be due to the onset of a bifunctional mechanism.

In the case of the supports with and without chlorine, Table 5 shows that only ring opening (selectivity between 5 and 22%) and isomerization (cyclohexane) products were formed. These results are in agreement with Galperin et al.,[46] who found that the selectivity to ring opening products was low with acid catalysts and that the main reaction path was MCP isomerization to cyclohexane followed by dehydrogenation. Under these conditions there was no formation of cracking products for lack of enough strong acid sites to crack the molecules. The incorporation of Ir drastically affected the selectivity. Cracking products were produced, and the selectivity to ring opening products is between 74 and 90% (Table 5).

The RO product distribution provides useful information about the reaction mechanism. A random (nonselective) cleavage would produce 2 mol of *n*-hexane and 2 mol of 2-methylpentane for each mole of 3-methylpentane (nC_6:2MP:3MP ratio of 2:2:1) as observed on small metallic particles. On the other hand, on larger metallic clusters, the cleavage of endocyclic substituted bonds is prohibited by steric hindrance and the theoretical product distribution ratio becomes 0:2:1.[47] If both mechanisms are present, the distribution ratios would be a combination of these previous values. In the case of the Ir/S*x* series, the experimental nC_6/3MP ratio was between 0.41 and 0.63 while the 2MP/3MP ratio was 1.04−1.29 (Table 5). This seems to indicate that an alternative mechanism is in operation. Several researchers found that MCP ring opening on Ir by a selective mechanism leads only to 2MP and 3MP as ring opening products[5,42,47−49] while the formation of cyclohexane and benzene required the presence of both the metal and acid sites.[50] The selectivity to all reaction products detected in the methylcyclopentane reaction can be seen in the Supporting Information (Table 2S).

Figure 6 shows the selectivity to RO and C_1−C_5 obtained in the MCP reaction as a function of the reaction rate of cyclopentane. The selectivity to C_1−C_5 increased with the reaction rate of cyclopentane, while the selectivity to RO products followed an inverse trend. These results were expected since C_1 and C_5 are produced mainly by hydrogenolysis. The selectivity to RO products shows that a higher hydrogenolytic activity leads to a lower selectivity to RO. These results point out that an adequate metal activity is necessary for the ring opening reaction. The selectivity to cracking products (C_1−C_5) was not directly proportional to the total acidity of the catalysts, the strong acidity, or the (strong + mild) acidity (even disregarding C_1 which is mainly produced by hydrogenolysis on the metal) (results not shown). The cracking

DOI: 10.1021/acs.energyfuels.7b00451
Energy Fuels 2017, 31, 5461−5471

Table 5. Reaction Rate of Methylcyclopentane; Selectivity to Cracking, Ring Opening (RO), and Isomerization Products; and C_6/3MP and 2MP/3MP Yield Ratios[a]

		selectivity (%)			ratio	
catalyst	reaction rate (μmol of MCP g^{-1} s^{-1})	cracking	RO	isomerization	nC_6/3MP	2MP/3MP
S30	0.645	–	5.1	94.9		
HCl/S30	0.734	–	8.4	91.6		
Ir/S30	8.366	9.9	90.1	–	0.62	1.04
S40	0.701	–	10.1	89.9		
HCl/S40	0.890	–	14.0	86.0		
Ir/S40	8.744	17.0	83.0	–	0.42	1.10
S60	0.901	–	9.6	90.4		
HCl/S60	1.046	–	12.1	87.9		
Ir/S60	9.623	11.8	87.8	0.4	0.57	1.29
S70	0.790	–	21.9	78.1		
HCl/S70	0.901	–	14.1	85.9		
Ir/S70	8.188	9.2	88.4	2.5	0.63	1.22
S80	0.879	–	22.1	77.9		
HCl/S80	0.990	–	5.3	94.7		
Ir/S80	10.190	25.7	74.3	–	0.41	1.28

[a]Reaction time = 10 min.

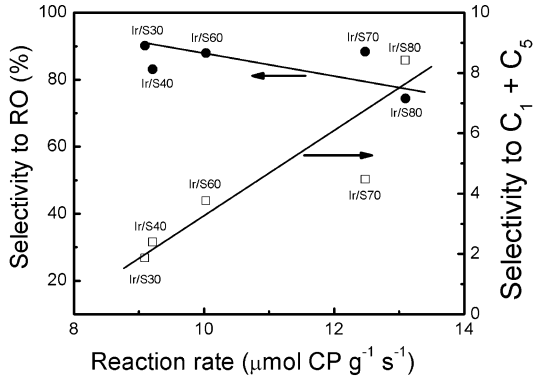

Figure 6. Selectivity to RO products and (C_1 + C_5), MCP reaction. Dependence on reaction rate.

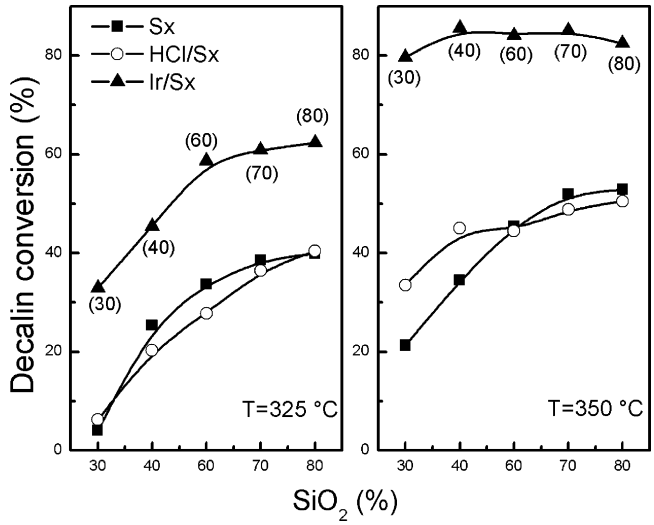

Figure 7. Conversion of decalin at 325 and 350 °C at 6 h as a function of SiO_2 content of the supports. Numbers in parentheses identify the support.

products are produced mainly on the strong acid sites of the catalyst, but the metal function plays an important role. The metal may be producing olefinic compounds that are cracked more easily.[45]

Figure 7 shows results of decalin conversion at 6 h reaction time at different reaction temperatures. At 325 °C conversion clearly increased with SiO_2 content in all three catalyst series. This can be due to the effect of the SiO_2 content on the acidity. The S60 support had the highest total acidity, but most of its sites had only low or moderate acid strength (Figure 2 and Table 3). At 350 °C all catalysts showed the same behavior observed at 325 °C, except for the Ir/S*x* series that showed conversion values between 79 and 85% in all cases. Moreover, the addition of HCl produced a major increase in conversion on the supports with low acidity (S30 and S40) but had no noticeable effect on the other supports.

Addition of Ir resulted in higher conversion values at both reaction temperatures. This effect was more marked in supports with low acidity in which SiO_2 and Al_2O_3 coexist separately. The increase of the conversion with the support acidity can be explained considering that the reaction of ring opening of decalin can occur through an acid monofunctional mechanism.[1,46] The addition of iridium drastically improved the conversion because it enabled the onset of a bifunctional metal−acid reaction mechanism,[1] with a lower energy activation barrier, in which the rate-controlling step is the ring contraction from six to five carbon atoms.[10] Given their high hydrogenolytic activity, these five-membered rings are easily opened over Ir. However, Ir has difficulties to isomerize decalin.[10,14,51] Therefore, the formation of decalin isomers could be due to a bifunctional mechanism controlled by the Brønsted acid sites.[5] At a higher reaction temperature, the conversion was higher because metal catalyzed reaction rates (hydrogenolysis and dehydrogenation) and acid catalyzed reaction rates (cracking and isomerization) are augmented at higher temperatures.[45]

The results in Figure 8 can be analyzed in order to infer the influence of the metal and the acid function on the decalin SRO. Figure 8 is a correlation between the results of decalin conversion and the reaction rate of CP (for the same catalyst). The decalin conversion as a function of the total acidity (determined by Py-TPD) of the catalysts is also plotted. As expected by the results reported in Figure 7, at 350 °C there

DOI: 10.1021/acs.energyfuels.7b00451
Energy Fuels 2017, 31, 5461−5471

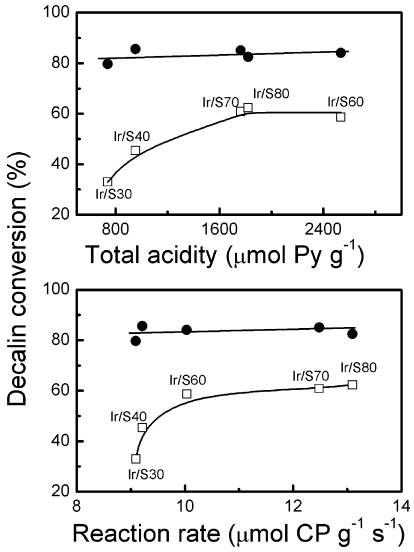

Figure 8. Ir/S*x* decalin conversion as a function of cyclopentane reaction rate and as a function of total acid sites. Reaction temperature: 325 (□) and 350 °C (●).

were no changes regarding decalin conversion as a function of the metal activity or acid sites of the catalysts. At 325 °C, decalin conversion as a function of the CP reaction rate and the amount of total acid sites shows an initial increase followed by a plateau. It can be concluded that, at 325 °C, decalin conversion depends on both the total acid and metal sites of the catalysts. The Ir/S60 catalyst that has the higher amount of acid sites failed to convert more decalin due to its lower hydrogenolytic activity compared to the Ir/S70 and Ir/S80 catalysts.

Following a previous work,[52] decalin reaction products were classified into cracking products (C_1−C_9 products), C_{10} ring opening products, ring contraction products (RC), and dehydrogenated products (PD, naphthalene and heavy dehydrogenated products). The composition of each group was included as Supporting Information. The yields of different groups of products obtained at both reaction temperatures are presented in Figures 9 and 10.

For each studied support, iridium addition produced materials with the highest yield of cracking, ring contraction, and ring opening products, at both 325 and 350 °C. The yield of dehydrogenated products (PD) at 350 °C was also higher on the Ir catalysts as compared to the S*x* and HCl/S*x* catalyst series. Moreover the addition of chlorine led to a higher PD yield at 350 °C. At 325 °C the PD yield was lower than 5% and no definite trend can be seen. Furthermore, the addition of Ir (with a high dehydrogenating activity) enhanced the formation of PD. It is important to point out that the PD yields at 350 °C on the Ir/S30 and Ir/S40 catalysts almost doubled those on the other Ir catalysts. The yield of RO products obtained with the S*x* and HCl/S*x* series was practically identical (at both temperatures) and increased markedly with the addition of Ir, confirming that the reaction proceeds by a bifunctional mechanism. In all the catalysts higher cracking yield, ring opening, and dehydrogenated products were obtained at 350 °C. On the contrary, the yield of ring contraction products decreased (except for S30).

The difference in the yield of cracking products (CR) at the two temperatures can be justified by the high activation energy of cracking reactions, which seems to be higher than the activation energy of the ring opening reaction.[18] For this reason

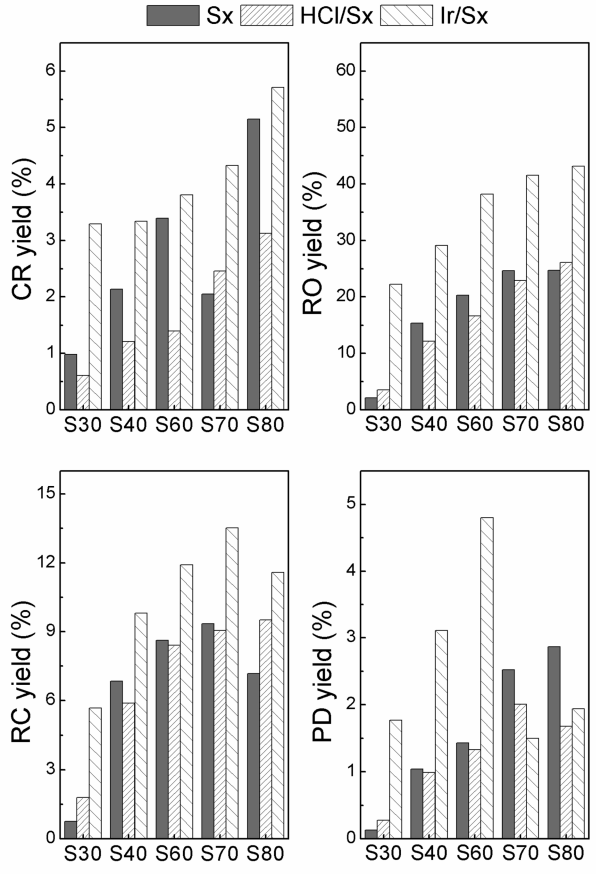

Figure 9. Yields of cracking products (CR), ring opening products (RO), ring contraction products (RC), and dehydrogenated products (PD), at 325 °C.

the $CR_{350\,°C}/CR_{325\,°C}$ yield ratio was greater than the $RO_{350\,°C}/RO_{325\,°C}$ yield ratio (except in the case of S30 support) (Table 6). Higher temperatures also favor the formation of dehydrogenated products since dehydrogenation is an endothermic reversible reaction.[24,45] This would justify a $PD_{350\,°C}/PD_{325\,°C}$ yield ratio higher than 1 (Table 6). Overall, these results correlate with similar conversion values obtained at 350 °C for all Ir catalysts. High reaction temperatures favored cracking and dehydrogenation reactions, and as a consequence, the selectivity to ring contraction products was decreased. The selectivity to ring contraction products was also low because they can be sequentially transformed into ring opening and cracking products.

The yield of RO products of decalin as a function of the reaction rate of cyclopentane and the total acidity are plotted in Figure 11. In contrast to the results of the MCP reaction (Figure 6), an increased RO yield is observed at higher values of the reaction rate of cyclopentane. The yield of RO products also increased with the total acidity at both reaction temperatures. The different results between decalin and MCP ring opening can be explained by taking into account the high stability of the fused double ring of decalin. This higher stability demands a stronger hydrogenolytic function to be opened. Alternatively, strong acid sites may enable the occurrence of ring contraction first, thus leading to a lower energy path for ring opening, given the easier opening of the C_5 ring. For this reason the RO product yield increased with the total acidity and the hydrogenolytic activity of the catalysts.

DOI: 10.1021/acs.energyfuels.7b00451
Energy Fuels 2017, 31, 5461−5471

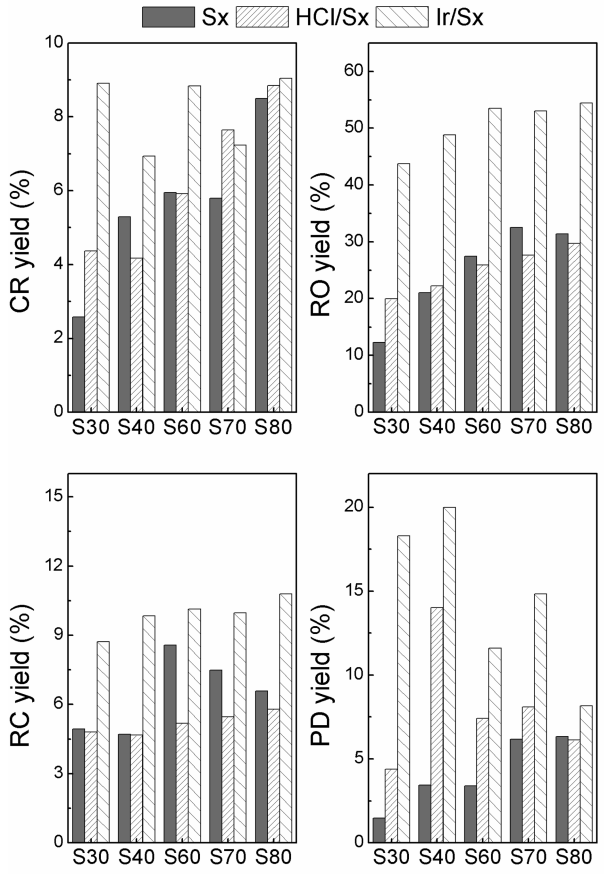

Figure 10. Yields of cracking products (CR), ring opening products (RO), ring contraction products (RC), and dehydrogenated products (PD), at 350 °C.

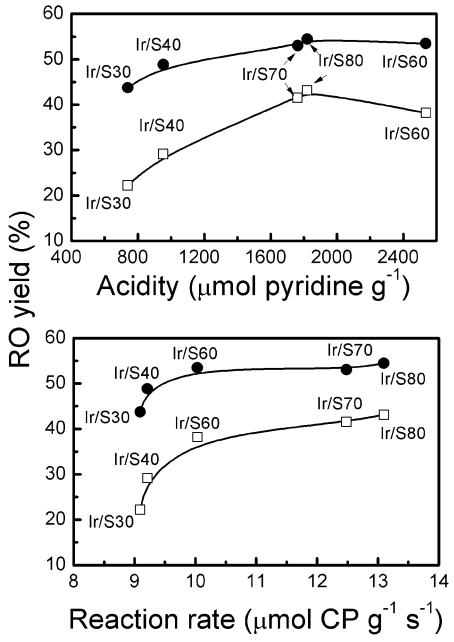

Figure 11. RO product yield as a function of total acidity and cyclopentane reaction rate. Reaction temperature 325 (□) and 350 °C (●).

Figure 12 shows the yield of RO + RC products as a function of the total acid sites/metal activity ratio (A/M). The total acid sites are expressed in μmol of Py g^{-1} from Table 3, while the metal activity is the reaction rate for cyclopentane hydrogenolysis (μmol of CP g^{-1} s^{-1}) reported in Figure 4. It can be seen that at both reaction temperatures the yield of RO + RC products increased with the A/M ratio at low A/M ratio until a plateau was reached at high A/M ratios. It is important to point out that the selectivity to RO + RC products or the selectivity to RO as a function of the A/M ratio followed the same tendency (results not shown). The selectivity to RO + RC at 325 °C was higher than the selectivity to RO + RC at 350 °C because the dehydrogenation and cracking reactions were more important at 350 °C (Figures 9 and 10). The higher yield of RO + RC at 350 °C compared to 325 °C was due to the higher activity of the catalysts at the higher reaction temperature (Figure 7). Piccolo et al.[23] reported a lineal increase of the selectivity to RO + RC products as a function of Brønsted acid sites/metal sites ratio using Ir/SiO_2–Al_2O_3 catalysts. Disregarding the Ir/S60 catalyst, the same tendency is seen here. These results clearly show that there was an optimum acid sites/metal activity ratio (A/M). At lower A/M ratios the isomerization reaction which leads to C_5 cycle isomers was low, and as a consequence the ring opening by hydrogenolysis was limited.

Table 6. Ratios of Different Yields at 350 and 325°C for Cracking, Ring Contraction, Ring Opening, and Dehydrogenation Products

catalyst	$CR_{350\,°C}/CR_{325\,°C}$	$RC_{350\,°C}/RC_{325\,°C}$	$RO_{350\,°C}/RO_{325\,°C}$	$PD_{350\,°C}/PD_{325\,°C}$
S30	2.6	6.5	5.7	11.3
HCl/S30	7.2	2.7	5.6	15.7
Ir/S30	2.7	1.5	2.0	10.3
S40	2.5	0.7	1.4	3.3
HCl/S40	3.4	0.8	1.8	14.2
Ir/S40	2.1	1.0	1.7	6.4
S60	1.8	1.0	1.4	2.4
HCl/S60	4.2	0.6	1.6	5.6
Ir/S60	2.3	0.9	1.4	2.4
S70	2.8	0.8	1.3	2.5
HCl/S70	3.1	0.6	1.2	4.0
Ir/S70	1.7	0.7	1.3	9.9
S80	1.7	0.9	1.3	2.2
HCl/S80	2.8	0.6	1.1	3.6
S30	1.6	0.9	1.3	4.2

DOI: 10.1021/acs.energyfuels.7b00451
Energy Fuels 2017, 31, 5461−5471

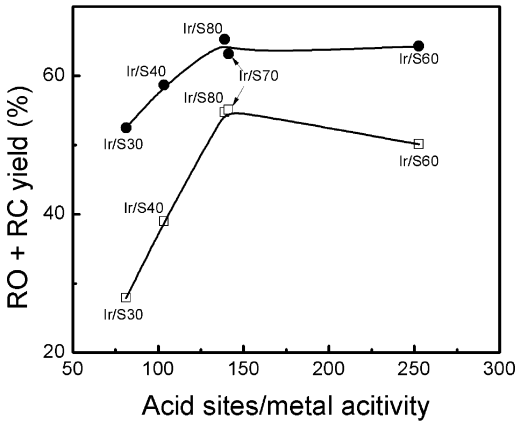

Figure 12. Yield of RO + RC products as a function of total acid sites/metal activity ratio obtained in the decalin reaction at 325 (□) and 350 °C (●).

On the other hand, at high A/M ratio the cracking reactions were favored, decreasing the yield of RO products.

The decalin used in the experiments had a concentration of 37.5% cis isomer and thus a cis/trans ratio of 0.6. It is obvious from the results shown in Table 7 that *cis*-decalin is highly

Table 7. *trans*- and *cis*-Decalin Concentration at 325 and 350 °C after 6 h of Reaction

	reaction temp 325 °C			reaction temp 350 °C		
catalyst	trans	cis	cis/trans ratio	trans	cis	cis/trans ratio
S30	47.6	48.3	1.01	51.1	27.7	0.54
HCl/S30	48.8	44.9	0.92	58.0	8.5	0.15
Ir/S30	59.0	8.0	0.14	18.5	1.9	0.10
S40	52.4	22.2	0.42	59.3	6.2	0.10
HCl/S40	52.0	27.8	0.53	53.3	1.7	0.03
Ir/S40	48.8	5.8	0.12	13.0	1.3	0.10
S60	52.2	14.1	0.27	48.3	6.3	0.13
HCl/S60	53.3	18.9	0.35	53.9	1.7	0.03
Ir/S60	37.3	3.9	0.10	14.7	1.3	0.09
S70	56.6	7.8	0.14	45.5	2.5	0.05
HCl/S70	52.1	11.5	0.22	49.7	1.5	0.03
Ir/S70	35.2	3.9	0.11	13.8	1.1	0.08
S80	55.4	4.3	0.08	45.6	1.6	0.04
HCl/S80	50.5	9.1	0.18	48.0	1.5	0.03
Ir/S80	34.1	3.6	0.11	16.1	1.4	0.09

reactive[53,54] and that cis to trans isomerization occurred.[55] The S30 and HCl/S30 catalysts at 325 °C are notable exceptions, with a higher *cis*/*trans*-decalin ratio than the original feed. *cis*-Decalin is known to be transformed more selectively to ring opening products than *trans*-decalin, which is mainly converted to cracked products.[53] Comparing the lowest *cis*/*trans*-decalin ratio at the end of the reaction (Table 7) with the yield of cracking products reported in Figures 9 and 10, no direct correlation can be found. In addition to the stereoisomerization taking place on acid sites, *cis*- to *trans*-decalin isomerization can occur on the metal sites through a hydrogenation−dehydrogenation mechanism.[56] A classical parameter to assess the extent of the stereoisomerization reaction of decalin is the trans/(cis + trans) ratio. For the Ir catalysts this ratio is between 0.88 and 0.93 for both reaction temperatures. This is the range of values reported for decalin opening over bifunctional catalysts.[18−20]

Results of the reaction test of decalin ring opening on different catalysts are comparatively included in Table 8. The

Table 8. Conversion of Decalin and Selectivity to RO Products Using Different Catalysts at the Same Reaction Conditions

catalyst	$T_{reaction}$ (°C)	conversion	selectivity to RO	ref
Ir/S30	325	32.9	67.4	this work
	350	79.7	54.9	
Ir/S40	325	45.4	64.2	this work
	350	85.6	57.1	
Ir/S60	325	58.7	65.1	this work
	350	84.1	63.7	
Ir/S70	325	60.9	68.2	this work
	350	85.1	62.3	
Ir/S80	325	62.3	69.1	this work
	350	82.5	66.0	
Ir(1 wt %)/HY	300	44.9	62.5	52
	350	70.8	54.12	
Ir(1.5 wt %)/HY	300	68.9	64.5	52
	350	73.5	55.9	
Rh(1 wt %)/S40	350	65.4	57.1	24

results put in evidence the superior performance of the Ir/S*x* catalysts for decalin SRO. At 350 °C the Ir (1 and 1.5 wt %) catalysts supported on zeolite HY failed to achieve the conversion and selectivity values of the Ir/S*x* catalysts. Moreover, using S40 as a support, the use of Ir instead of Rh significantly increased the conversion and selectivity to RO products. It is also seen in Table 8 that a slight decrease in selectivity to RO was produced in the Ir/S*x* series when the reaction temperature was increased from 325 to 350 °C. Nevertheless, the higher conversion was accompanied by a higher yield of ring opening products.

Because of differences in the reaction conditions, it is difficult to make a comparison with the results of other authors and a given degree of uncertainty is attached to any conclusion drawn. It may be mentioned, nonetheless, that Rabl et al.[20] used Ir(2.9 wt %)/Na,HY as a catalyst for reacting *cis*-decalin and reported a selectivity to ring opening products and open-chain decanes close to 63%, at a value of 86% conversion. These results were obtained at 300 °C with *cis*-decalin at 5.2 MPa hydrogen pressure in a continuous fixed-bed reactor. This feed results in a higher selectivity toward ring opening products in comparison to a mixture of *cis*-decalin and *trans*-decalin.

CONCLUSIONS

A comparison was made of the catalytic properties of different SiO_2−Al_2O_3 supports of varying SiO_2 content, impregnated with Ir (1%) and with or without the addition of HCl, for the selective ring opening (SRO) of decalin.

A linear correlation was found between the MCP RO reaction rate and the catalyst acidity for SiO_2−Al_2O_3 support with and without Cl addition. The addition of Ir was found to increase the reaction rate by an order of magnitude and to deeply alter product distribution. The nC_6/3MP and 2MP/3MP ratios showed that the reaction proceeded through a partially selective mechanism. Furthermore, at higher metal activities (measured as the CP hydrogenolysis reaction rate), the selectivity toward C_1+ C_5 (which are hydrogenolysis

DOI: 10.1021/acs.energyfuels.7b00451
Energy Fuels 2017, 31, 5461−5471

products) increased while the selectivity to RO products decreased.

Decalin conversion appears to be strongly influenced by the acidity and metallic function of the catalyst. The HCl/S*x* series showed almost the same yield of ring opening products as the chlorine-free supports. Beyond these general trends, the addition of HCl produced different results depending on the support used.

Iridium addition contributed to the formation of ring opening and ring contraction products. The yield of cracking and dehydrogenation products was also increased. The addition of Ir had a more important effect than the addition of HCl.

From these decalin ring opening tests it can be concluded that the most suitable supports are those with a high percentage of SiO_2 (70 and 80 wt %) with a medium total acidity and the absence of isolated alumina groups. Catalysts with low acidity (Ir/S30) or high acidity (Ir/S60) have lower selectivity to RO + RC products due to the formation of dehydrogenated or cracking products.

The increase in reaction temperature favored the formation of cracking, ring opening, and dehydrogenated products at the expense of ring contraction products.

■ ASSOCIATED CONTENT

Supporting Information

The Supporting Information is available free of charge on the ACS Publications website at DOI: 10.1021/acs.energyfuels.7b00451.

Figures 1S−5S, representative TEM images of Ir supported catalysts; Tables 1S and 2S, reaction rate and selectivity to reaction products obtained on cyclopentane and methylcyclopentane reaction on Ir/S*x* catalysts; decalin reaction products classification (PDF)

■ AUTHOR INFORMATION

Corresponding Author

*E-mail: pieck@fiq.unl.edu.ar.

ORCID

Silvana A. D'Ippolito: 0000-0002-5104-3364

Notes

The authors declare no competing financial interest.

■ REFERENCES

(1) Du, H.; Fairbridge, C.; Yang, H.; Ring, Z. *Appl. Catal., A* **2005**, *294*, 1−21.
(2) Cooper, B. B. H.; Donnis, B. B. L. *Appl. Catal., A* **1996**, *137*, 203−223.
(3) Calemma, V.; Ferrari, M.; Rabl, S.; Weitkamp, J. *Fuel* **2013**, *111*, 763−770.
(4) Daage, M.; McVicker, G. B.; Touvelle, M. S.; Hudson, C. W.; Klein, D. P.; Cook, B. R.; Chen, J. G.; Hantzer, S.; Vaughan, D. E. W.; Ellis, E. S. *Stud. Surf. Sci. Catal.* **2001**, *135*, 159.
(5) McVicker, G. B.; Daage, M.; Touvelle, M. S.; Hudson, C. W.; Klein, D. P.; Baird, W. C., Jr.; Cook, B. R.; Chen, J. G.; Hantzer, S.; Vaughan, D. E. W.; Ellis, E. S.; Feely, O. C. *J. Catal.* **2002**, *210*, 137−148.
(6) Kubička, D.; Kumar, N.; Maeki-Arvela, P.; Tiitta, M.; Niemi, V.; Karhu, H.; Salmi, T.; Murzin, D. Y. *J. Catal.* **2004**, *227*, 313−327.
(7) Mouli, K. C.; Sundaramurthy, V.; Dalai, A. K.; Ring, Z. *Appl. Catal., A* **2007**, *321*, 17−26.
(8) Nassreddine, S.; Massin, L.; Aouine, M.; Geantet, C.; Piccolo, L. *J. Catal.* **2011**, *278*, 253−265.
(9) Do, P. T. M.; Crossley, S.; Santikunaporn, M.; Resasco, D. E. *Catalysis* **2007**, *20*, 33−64.
(10) Moraes, R.; Thomas, K.; Thomas, S.; Van Donk, S.; Grasso, G.; Gilson, J.-P.; Houalla, M. *J. Catal.* **2013**, *299*, 30−43.
(11) Alzaid, A. H.; Smith, K. J. *Appl. Catal., A* **2013**, *450*, 243−252.
(12) Arve, K.; Mäki-Arvela, P.; Eränen, K.; Tiitta, M.; Salmi, T.; Murzin, D. Yu. *Chem. Eng. J.* **2014**, *238*, 3−8.
(13) Carter, J. L.; Cusumano, J. A.; Sinfelt, J. H. *J. Catal.* **1971**, *20*, 223−229.
(14) Walter, C. G.; Coq, B.; Figueras, F.; Boulet, M. *Appl. Catal., A* **1995**, *133*, 95−102.
(15) Del Angel, G.; Coq, B.; Dutartre, R.; Figueras, F. *J. Catal.* **1984**, *87*, 27−35.
(16) Zimmer, H.; Paal, Z. *J. Mol. Catal.* **1989**, *51*, 261−278.
(17) Nassreddine, S.; Casu, S.; Zotin, J. L.; Geantet, C.; Piccolo, L. *Catal. Sci. Technol.* **2011**, *1*, 408−412.
(18) Rabl, S.; Haas, A.; Santi, D.; Flego, C.; Ferrari, M.; Calemma, V.; Weitkamp, J. *Appl. Catal., A* **2011**, *400*, 131−141.
(19) Santi, D.; Holl, T.; Calemma, V.; Weitkamp, J. *Appl. Catal., A* **2013**, *455*, 46−57.
(20) Rabl, S.; Santi, D.; Haas, A.; Ferrari, M.; Calemma, V.; Bellussi, G.; Weitkamp, J. *Microporous Mesoporous Mater.* **2011**, *146*, 190−200.
(21) Marcilly, C. *Catalyse Acido-Basique: Application au Raffinage et à la Pétrochimie*; Ed. Technip: 2003; Vol. *1*, Chapter 4.
(22) Santikunaporn, M.; Alvarez, W. E.; Resasco, D. E. *Appl. Catal., A* **2007**, *325*, 175−187.
(23) Piccolo, L.; Nassreddine, S.; Toussaint, G.; Geantet, C. *ChemSusChem* **2012**, *5*, 1717−1723.
(24) D'Ippolito, S. A.; Especel, C.; Vivier, L.; Epron, F.; Pieck, C. L. *Appl. Catal., A* **2014**, *469*, 532−540.
(25) D'Ippolito, S. A.; Especel, C.; Vivier, L.; Pronier, S.; Epron, F.; Pieck, C. L. *J. Mol. Catal. A: Chem.* **2015**, *398*, 203−214.
(26) Hensen, E. J. M.; Poduval, D. G.; Ligthart, D. A. J. M.; van Veen, J. A. R.; Rigutto, M. S. *J. Phys. Chem. C* **2010**, *114*, 8363−8374.
(27) Lecarpentier, S.; Van Gestel, J.; Thomas, K.; Gilson, J.-P.; Houalla, M. *J. Catal.* **2008**, *254*, 49−63.
(28) Kubicka, H. *J. Catal.* **1968**, *12*, 223−237.
(29) Carvalho, L. S.; Conceição, K. C. S.; Mazzieri, V. A.; Reyes, P.; Pieck, C. L.; Rangel, M. C. *Appl. Catal., A* **2012**, *419−420*, 156−163.
(30) D'Ippolito, S. A.; Vera, C. R.; Epron, F.; Samoila, P.; Especel, C.; Marécot, P.; Gutierrez, L. B.; Pieck, C. L. *Appl. Catal., A* **2009**, *370*, 34−41.
(31) Li, Z.; Meng, F.; Ren, J.; Zheng, H.; Xie, K. *Chin. J. Catal.* **2008**, *29*, 643−648.
(32) Hao, F.; Zhong, J.; Liu, P. L.; You, K. Y.; Wei, C.; Liu, H. J.; Luo, H. A. *J. Mol. Catal. A: Chem.* **2011**, *351*, 210−216.
(33) Pawelec, B.; Venezia, A. M.; La Parola, V.; Cano-Serrano, E.; Campos-Martin, J. M.; Fierro, J. L. G. *Appl. Surf. Sci.* **2005**, *242*, 380−391.
(34) Sharma, L. D.; Kumar, M.; Saxena, A. K.; Chand, M.; Gupta, J. K. *J. Mol. Catal. A: Chem.* **2002**, *185*, 135−141.
(35) Mironenko, R. M.; Belskaya, O. B.; Talsi, V. P.; Gulyaeva, T. I.; Kazakov, M. O.; Nizovskii, A.; Kalinkin, A. V.; Bukhtiyarov, V. I.; Lavrenov, A. V.; Likholobov, V. A. *Appl. Catal., A* **2014**, *469*, 472−482.
(36) Gates, B. C.; Katzer, J. R.; Schuit, A. G. C. *Chemistry of Catalytic Processes*; McGraw-Hill: New York, 1979; pp 184−324.
(37) Carvalho, L. S.; Pieck, C. L.; Rangel, M. C.; Fígoli, N. S.; Vera, C. R.; Parera, J. M. *Appl. Catal., A* **2004**, *269*, 105−116.
(38) Selli, E.; Forni, L. *Microporous Mesoporous Mater.* **1999**, *31*, 129−140.
(39) Pamphile-Adrián, A. J.; Florez-Rodriguez, P. P.; Passos, F. B. *J. Braz. Chem. Soc.* **2016**, *27* (5), 958−966.
(40) Huang, Y. J.; Xue, J.; Schwarz, J. A. *J. Catal.* **1988**, *111*, 59−66.
(41) Subramanian, S.; Schwarz, J. A. *Appl. Catal.* **1991**, *74*, 65−81.
(42) Gault, F. G. *Adv. Catal.* **1981**, *30*, 1−95.
(43) Biloen, B.; Helle, J.; Verbeek, H.; Dautzenberg, F.; Sachtler, W. *J. Catal.* **1980**, *63*, 112−118.
(44) Djeddi, A.; Fechete, I.; Garin, F. *Appl. Catal., A* **2012**, *413−414*, 340−349.

DOI: 10.1021/acs.energyfuels.7b00451
Energy Fuels 2017, 31, 5461−5471

(45) Parera, J. M.; Figoli, N. S. In *Catalytic Naphtha Reforming: Science and Technology*; Antos, G. J., Aitani, A. M., Parera, J. M., Eds.; Marcel Dekker Inc.: New York, 1995; Chapter 3.
(46) Galperin, L. B.; Bricker, J. C.; Holmgren, J. R. *Appl. Catal., A* **2003**, *239*, 297−304.
(47) Maire, G.; Plouidy, G.; Prudhomme, J. C.; Gault, F. G. *J. Catal.* **1965**, *4*, 556−569.
(48) van Senden, J. G.; van Broekhoven, E. H.; Wreesman, C. T. J.; Ponec, V. *J. Catal.* **1984**, *87*, 468−477.
(49) Barron, Y.; Maire, G.; Muller, J. M.; Gault, F. G. *J. Catal.* **1966**, *5*, 428−445.
(50) Dees, M. J.; Bol, M. H. B.; Ponec, V. *Appl. Catal.* **1990**, *64*, 279−295.
(51) Haas, A.; Rabl, S.; Ferrari, M.; Calemma, V.; Weitkamp, J. *Appl. Catal., A* **2012**, *425*−*426*, 97−109.
(52) D'Ippolito, S. A.; Gutierrez, L. B.; Pieck, C. L. *Appl. Catal., A* **2012**, *445*−*446*, 195−203.
(53) Santikunaporn, M.; Herrera, J. E.; Jongpatiwut, S.; Resasco, D. E.; Alvarez, W. E.; Sughrue, E. L. *J. Catal.* **2004**, *228*, 100−113.
(54) Sousa-Aguiar, E. F.; Mota, C. J. A.; Valle Murta, M. L.; Pinhel da Silva, M.; Forte da Silva, D. *J. Mol. Catal. A: Chem.* **1996**, *104*, 267−271.
(55) Schucker, R. C. *J. Chem. Eng. Data* **1981**, *26*, 239−241.
(56) Moraes, R.; Thomas, K.; Thomas, S.; van Donk, S.; Grasso, G.; Gilson, J.-P.; Houalla, M. *J. Catal.* **2012**, *286*, 62−77.

DOI: 10.1021/acs.energyfuels.7b00451
Energy Fuels 2017, 31, 5461−5471